Environment. Technology. Resources. Rezekne, Latvia
Proceedings of the 14th International Scientific and Practical Conference. Volume 3, 297-305

Features of Color Laser Marking on Metals

Nikolay Todorov Dolchinkov
Vasil Levski National Military University, Veliko Tarnovo, Bulgaria
National Research University "Moscow Power Engineering Institute", Moscow, Russia
Veliko Tarnovo, Bulgaria
n_dolchinkov@abv.bg

Teodor Petrov
Vasil Levski National Military University, Veliko Tarnovo, Bulgaria
Veliko Tarnovo, Bulgaria
Tedo089@abv.bg

Georgi Petrov
Vasil Levski National Military University, Veliko Tarnovo, Bulgaria
Veliko Tarnovo, Bulgaria
gpetrov129@abv.bg

Christian Tolev
Vasil Levski National Military University, Veliko Tarnovo, Bulgaria
Veliko Tarnovo, Bulgaria
kris997@abv.bg

Emanuil Dimitrov
Vasil Levski National Military University, Veliko Tarnovo, Bulgaria
Veliko Tarnovo, Bulgaria
emkoto99@abv.bg

Abstract. **In the research carried out at the Rezekne Academy of Technology, the technology for color laser marking on chromium-nickel base and other metal bases was used in industrial production from the point of view of the repeatability and stability of the produced color markings. The study and research was done during the Erasmus internship by the authors at the Academy of Technology in Rezekne, Latvia. For this purpose, an AISI 304 color palette consisting of fifteen colors was developed and implemented. After the practical experiments, the dependence of the obtained colors on the various parameters of the laser processing was analyzed. The resulting colors were then tested using optical, scanning electron and atomic force microscopy, and the configuration of the oxide films was determined by Raman spectroscopy. The resulting colors are of appropriate uniformity, brightness and cover almost all spectral zones, and the resulting colors are of many times better quality than other metallic bases. A color standardization and palette repeatability test was also performed by evaluating the reflectance spectra of the formed colors. The color palette demonstrated high repeatability for all but one particular color. In parallel, the stability of the color markings was studied in terms of environmental, mechanical and chemical resistance. The resulting colors show high resistance to most environmental conditions; however, exposure to very high temperatures and extreme humidity (100 °C, 90%) and to low temperatures and extreme humidity (-40 °C, 90%) results in degradation of several colors. Colored brands show high hardness and excellent mechanical resistance to external influences and exceptional resistance to various chemicals, except for acid solutions and salts.**

Keywords: color marking; laser; marking; power; speed.

I. Introduction

The marking of the various materials is an essential part of the production cycle, which provides the necessary information about the product and serves as a marketing tool to attract the attention of consumers to a particular product. Although various types of markings are applied to products, permanent markings are preferred [1], [2]. A variety of techniques can be used to create a permanent mark, including etching, electrochemical etching, engraving, dot etching, and laser marking. Nowadays, laser marking is widely used in various sections of the production line for a variety of applications to create high-quality permanent marks. The laser marking method is effective, non-contact and applies to both metallic and non-metallic surfaces. In addition, it requires no additional additives or solvents and produces no waste; thus, it is environmentally sustainable. Additionally, laser surface coloring is possible using color laser marking technology, which is the focus of this article. Color laser marking has been known for a long time, so many studies have been conducted on the use of different types of laser sources, the influence of environmental conditions on the results, and the analysis of the physical and chemical properties of surfaces before and after laser treatment. A technique for laser marking substrates such as ceramics, glass, plastic and metal was proposed by Axtell [3], [4]. In the laboratory of the Chinese scientist Li se. obtained a comprehensive view of the process of oxide formation during the interaction of an ultraviolet laser beam with stainless steel in air [5]. Modeling of coloring of stainless steel surfaces with

Print ISSN 1691-5402
Online ISSN 2256-070X
https://doi.org/10.17770/etr2023vol3.7222

colored pixels by heating the surface using a laser was carried out by Lehmuchero in his laboratory. [6]. Dusser and his team demonstrated the achievement of material modifications using ultrafast laser pulses by creating polarization-dependent structures that can create specific color designs [7]. Color laser marking technology for coloring metals has also been researched at Gorny's research center. [8], [9]. The famous scientist Visco and his team researched a method for coloring metal surfaces, in which nanosecond laser pulses form small-scale periodic structures [6]. Liu and his team investigated the recent developments of laser technologies for surface coloring and three specific physical mechanisms for color generation, which are the thin-film surface oxidation effect, laser-induced periodic surface structures (LIPSSs), and laser-induced nanoparticles and nanostructures [7], [10], [11].

II. MATERIALS AND METHODS

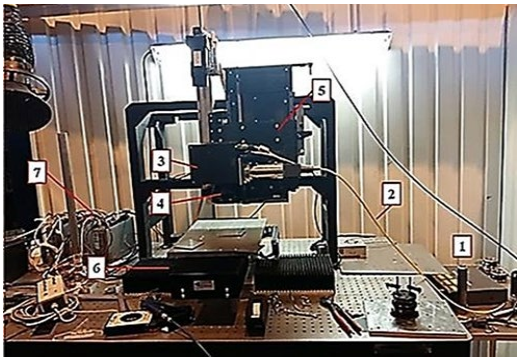

Figure 1: The configuration of the laser processing system.

Setting and parameters of the laser procedure Stainless steel contains chromium in its composition, which provides chemical stability and high heat resistance of the alloy and makes it suitable for use in the laser process. AISI 304 stainless steel plates with a thickness of 2 mm and initial roughness level Rz = 8.42 μm, reflectivity R (λ=1.06 μm) = 0.75, thermal diffusivity a = 3x10-6 are used in this study. m2/s, thermal conductivity k = 37 W/mK, melting point = 1800 °C and boiling point = 3145 °C. At the initial stage, the surfaces were cleaned with acetone to avoid any contamination or stains. A nanosecond pulse ytterbium fiber laser supplied by IPG Photonics Corporation <τ<200 ns at a repetition rate of 1.6 was selected as the source of laser radiation with a wavelength of 1055<λ<1075 nm generating pulses of 4 seconds duration <f<1000kHz. The configuration of the laser processing system developed for scribing and marking purposes is presented in Fig. 1 and consists of 1) IPG Photonics nanosecond fiber laser, 2) fiber optic transfer, 3) SCANLAB scanning system, 4) 100 mm objective, 5) Neff-Wiesel linear drive for vertical movement, 6) XY coordinate stage, 7) Kollmorgen ACD servo drives.

A fiber pulsed ytterbium laser was emitted and fed into a collimating system via an optical fiber to form a parallel beam output. A dual-axis galvanometer scanning system (hurrySCAN II 14 digital scanning head from SCANLAB corp.) was installed to move along the X and Y axes. A focusing lens with a focal distance 100 mm [11], [12]. Additional horizontal movements and vertical movements can be performed using a multi-axis linear motor coordinate stage, which allows the extension of the working space to 250×250 mm. Laser radiation parameters and scan speed can be changed using the developed labVIEW code. Also, all vertical and horizontal movements can be controlled by the same code.

A focused laser beam with a diameter d0 moving at a speed Vsc and a pulse repetition rate f irradiates a sample surface along a line (Fig. 2). When one scan line is completed with an overlap, the laser beam continues along the Y axis along the next line with an overlap Ly(%), characterized by the hatch spacing H, where P is the laser power and d0 is the spot diameter. A laser beam diameter is needed to calculate the power density of the laser radiation. In this study, the diameter of the laser beam is 40 μm.

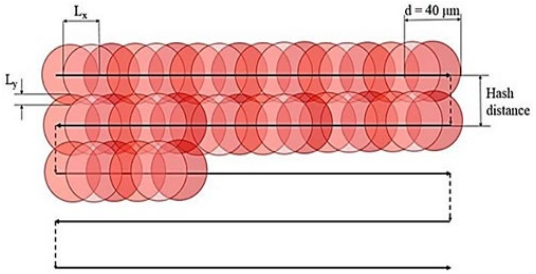

Figure 2 Focused laser beam.

Color palette development

The color laser marking process involves sequential melting and solidification of the material, which results in oxidation and nitriding of the material surface. The final surface and oxide film formation is the result of repeated pulsed laser operation, which varies depending on the heat of the laser and the overlap value of the laser pulses [13], [14], [15]. The result of the relief and color of the surface is affected by almost all parameters of the laser source. In this study, the dependence of the obtained colors on the scanning speed, laser power, pulse duration and laser pulse frequency is investigated. The study of the dependence of the resulting color on the surface relief is not the aim of this study.

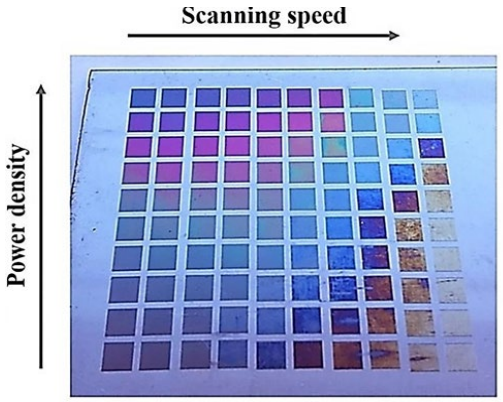

Figure 3: Dependence of obtained colors on power and speed.

The result shows that with increasing power the colors do not change significantly and only the parametric window moves to higher values of the scan rate for each color [1], [16]. Given that greater performance can be obtained at higher intensities, the next step was to investigate the dependence of color on scan rate with a maximum continuous power of 20 W available at the same parameters of frequency, hatch spacing and duration of the impulse. Initially, the scanning speed was changed from 450 to 850 mm/s with a step of 10 mm/s, and then from 50 to 150 mm/s with the same step. The results are presented in Fig. 4.

Figure 4: Obtaining a color palette at different speeds.

As shown in fig. 4, at a low scan speed, only dark gray colors appear, while as the scan speed increases, the colors vary in the following order: dark green, dark violet, wine red, orange, light green, gold, and light blue.

To investigate the dependence of colors on the frequency of laser pulses, the experiment was carried out with I0=1.6-108 W/cm2, r =100 ns, H=0.01 mm, Vsc=450-1200 mm /s with step 50 mm/s and a changing frequency that changes from top to bottom every two lines, 100, 200, 500 and 1000 kHz respectively. Fig. 5 shows the dependence of the color on the scan rate for different frequencies.

Figure 5 shows the dependence of the produced color on the scanning speed for different frequencies (I0 =1. 6·108 W/ cm^2, τ=100 ns, H=0.01 mm, Vsc =450- 1200 mm /s, f =100 kHz: lines No. 1, 2 ; f= 200 kHz: lines No. 3, 4 ; f=500 kHz: lines No. 5 ,6 ; f=1000 kHz: lines No. 7, 8 .

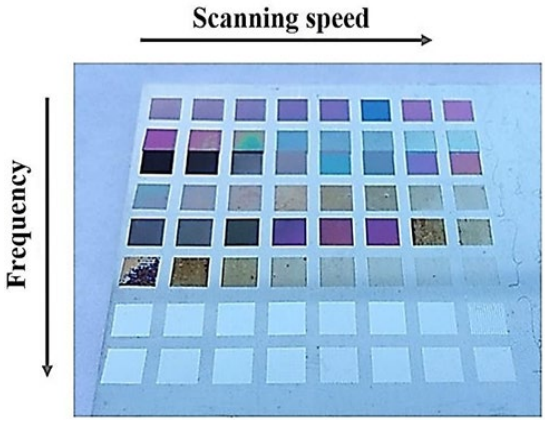

Figure 5. The dependence of the produced color on the scanning speed.

The test result revealed that specific colors such as light pink, aquamarine or bright purple can be obtained with higher frequency modes. At f=1000 kHz, only silver colors are formed for the entire scan rate range; hence, the parametric color window could not be produced at the mentioned frequency, although it could be assimilated into a final palette to produce white or silver due to its fast production speed.

The experiment to study the dependence of colors on the pulse duration was carried out with two different power densities I_0=0.8x10^7 and I_0=1.6x10^7 W/cm^2 and two different pulse durations r=4 and r=8 ns with scan speed Vsc=50 - 200 mm/s with step 10 mm/s and H=0.01 mm. The test result is shown in Fig. 6.

Figure 6 shows the dependence of the produced color on the scan rate for different pulse durations (Vsc=50-200 mm/s, H=0.01 mm, f=60 kHz, lines № 1, 2: τ=4 ns, I_0=0.8x10^8 W/cm^2; lines № 3, 4: τ=4 ns, I_0=1.6x10^8 W/cm^2; lines № 5, 6: τ=8 ns, I_0=0,8x10^7 W/cm^2; line № 7: τ=8 ns, I_0=16x10^8 W/cm^2).

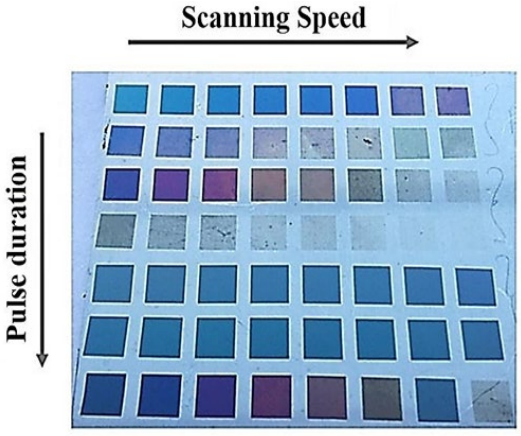

Figure 6. The dependence of the produced color on the scan rate for the different pulse durations.

As can be seen from fig. 6, the duration of the pulse has a significant effect on the color. The sequence of colors, hues and surface roughness under the color are different for shorter and longer pulse durations. For a longer duration pulse (r=20 ns), visually the colors are glassy and the material underneath is smoother compared to the shorter duration pulses. In contrast, for shorter pulses, the parametric window is shifted to the scan rate with lower values, which reduces the marking efficiency.

Almost the same color dependence is observed for pulse durations of 4 ns and 8 ns; however, with a pulse duration of 8 ns, the scan rate is higher and the resulting colors are more consistent. Based on the analysis performed, the number of pulses per spot (Nx, Ny) and the power density (I_0) were selected to develop a color palette with fifteen different shades for AISI 304 stainless steel [3], [7], [17], [18]

Analysis of the obtained structures

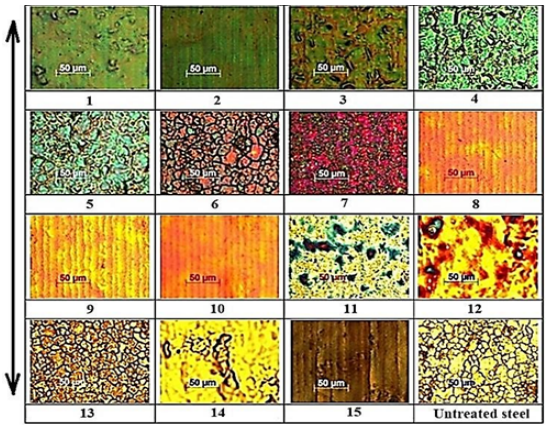

Figure 7. Micrographs of the color palette for AISI 304 stainless steel.

Optical microscopy was used to examine the microstructure of the developed colors and to analyze the oxide film structure of the color palette. The micrographs of each produced color and of the untreated surface are shown in Fig. 7.

Evaluation of the microimages shows that the created color patterns with large overlap, i.e., with large Nx and Ny values, are composed of distinct regions of different colors. In addition, the structure of the oxide film will be different depending on the overlapping and laser processing mode.

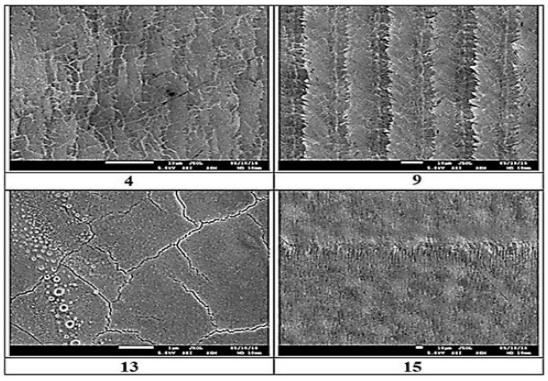

Figure 8. SEM images of the samples.

Some samples, including samples No. 8, 9, 10, 15, have a pronounced bar microstructure, while samples No. 11, 12, 14 have an irregular microstructure, and samples No. 6 and 7 have a granular structure. For a more detailed study of the structures, scanning electron microscopy (SEM) images of some samples were taken with an electron beam acceleration voltage of 5kV (Fig. 8).

The structures were also investigated by atomic force microscopy (AFM) operating in contact mode. The surface profile of specimen №9 and the 3D plane are shown in Fig. 9.

In fact, the sample has a periodically repeating relief that corresponds to the scanning geometry. The maximum and average roughness heights are nearly 2.6 and 1.5 µm, respectively, which is quite small compared to the material surface roughness (Rz = 8.42 µm).

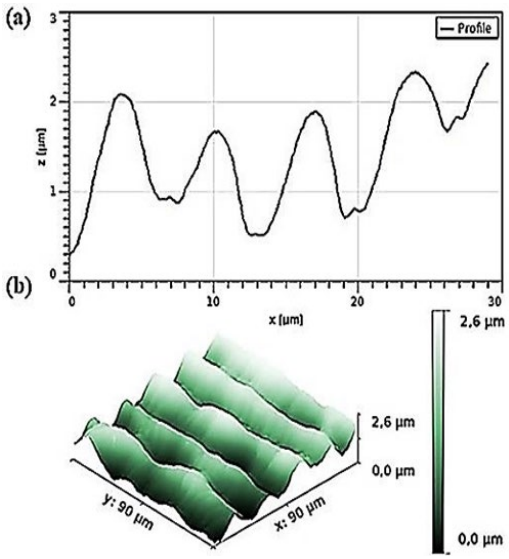

Figure 9: Profile of the studied material.

To determine the chemical composition of the obtained samples in this study, the Raman scattering method was used [5], [16], [18], [19]. A solid-state laser was used for the Raman scattering analysis. It initiates scattering on the surface of sample #9 with a wavelength of 532 nm and an output power of 1 mW (Fig. 10). A Lorentz fit function was applied to the plot to accurately characterize the position of the peaks. Seven Lorentzian peaks at 288, 332, 390, 541, 634, 674 and 715 cm-1. $FeCr_2O_4$ has eigenphonon modes that coincide with 541, 634, 674 cm-1; therefore, this means the presence of $FeCr_2O_4$ in the produced films. The peaks at 288, 332, 390 and 715 cm-1 are associated with the existence of maghemite (Fe_2O_3) or a maghemite-rich region that may exist due to the oxide film in addition to the virgin steel.

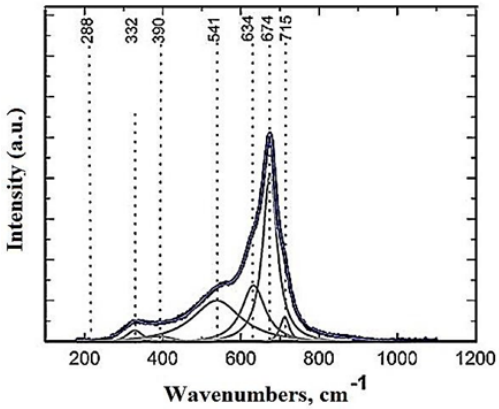

Figure 10: Dependence of intensity on distance.

III. RESULTS AND DISCUSSION

The quality of the coating is essential for industrial production and must meet the requirements of standardization organizations, manufacturers and users [1], [5], [11]. The produced colors were tested for repeatability and stability in terms of environmental, mechanical and chemical resistance.

Repeatability is a crucial factor in color coatings in the sense that the same color can be reproduced in different production runs. Color determination is done by analyzing the reflectance and transmission spectra of the objects. In this research work, the standard CIE RGB coordinate space is used to control the colors of the samples, in which the red (R), green (G) and blue (B) components of the flux form the coordinates [8]. The additive rule in Eq. 1 is used to define colors in this system [7].

$$C = \acute{r}\,\bar{R} + \acute{g}\,\bar{G} + \acute{b}\,\bar{B} \quad (1)$$

Where $\bar{R}$, $\bar{G}$, $\bar{B}$ are the units of the respective primary colors, and r , g , b are the number of units of each primary color required to construct the particular color C. The relative color coordinates can be calculated similarly to those in the CIE XYZ system via Eq. 2-4 [4].

$$r = r / (r + g + b) \quad (2)$$

$$g = g / (r + g + b) \quad (3)$$

$$b = b / (r + g + b) \quad (4)$$

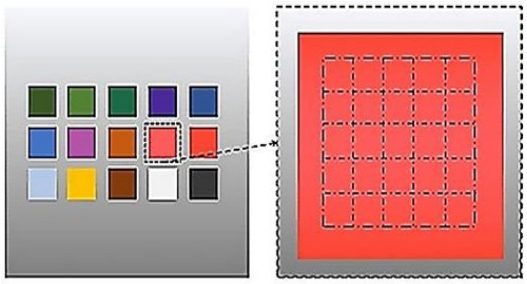

Figure 11. Matrix for conducting the tests.

The reflectance spectra of each color are needed to calculate the color coordinates. As shown in fig. 11, each color square is divided into 25 areas; therefore, the final spectrum is the average spectrum of the selected areas.

Depending on the type of peaks that appear in the wavelength, four groups of spectra can be defined. The first group (Fig. 12a) are flat spectra that do not have obvious peaks in the wavelength range and their initial appearance resembles the spectra of untreated steel. In the second group (Fig. 12b), one clear peak is observed between 500 and 700 nm. In the third group, two peaks are observed around 420 and 550 nm, respectively (Fig. 12c). In the last group (Fig. 12d), the peaks are broadened compared to the previous group. Interference effects in the denser oxide film and surface staining are suggested to be responsible for the peaks. A program was developed in LabVIEW to calculate the color coordinates in the CIE RGB space for each sample [3], [8], [20], [21].

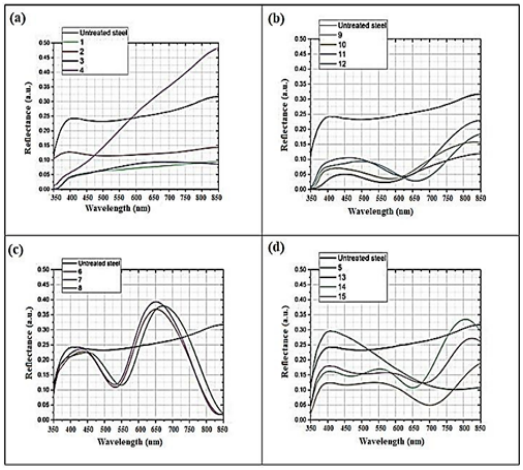

Figure 12: Spectra of the investigated material.

To investigate the repeatability, twenty color palettes were made, six of which are shown in Fig. 13.

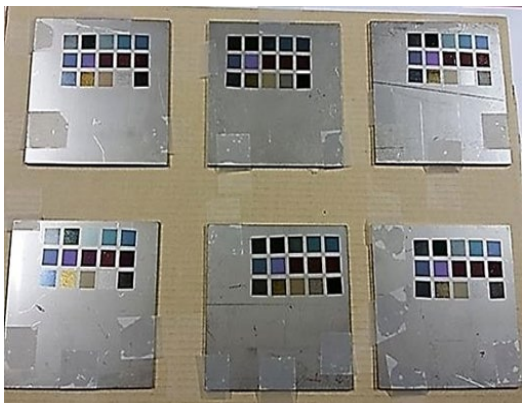

Figure 13. Six identical color palettes produced with the same laser processing parameters.

The difference in the colors of the palettes determines the repeatability of the colors obtained by applied laser technology. The International Commission on Illumination defines the color difference standard using the definition of the Delta E concept, which represents the evaluation of the change in the visual perception of two specified colors [6], [10]. In this study, the concept of delta E was used to estimate the color difference [6], [12], [22]. For color repeatability purposes, delta E = 2 is typically used. The average value of delta E was calculated using MATLAB code for all samples of the same color, which are presented in Fig. 14.

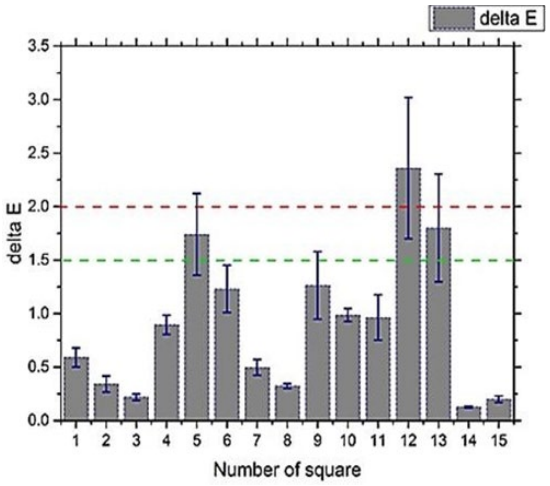

Figure 14. Delta E values of fifteen different colors averaged over ten samples.

The green line is the minimum delta E value perceived by the human eye. The red line is the maximum delta E value allowed in production.

According to fig. 14, the repeatability of all colors is satisfactory, making them suitable for use in the production line. The majority of color squares (№ 1, 2, 3, 7, 8, 14, 15) have superior delta E, so color variation is not noticeable even under close observation by an experienced observer. Samples №. 4, 6, 10 and 11 have acceptable delta E values in the sense that the color difference can only be detected by an experienced observer under suitable lighting conditions. Square #9 still has a satisfactory delta E value that is acceptable for production use. Squares №. 5 and 13 have higher average delta E values, which can be related to the corner effect [2], [12], although these colors can still be inserted into the color palette because they were not visually established differences between samples. Square №12 has the largest delta E value and correspondingly the lowest repeatability, which means that a casual observer can notice the difference. Therefore, this color cannot be recommended for further use. This problem can be solved by adjusting the laser processing parameters or by choosing different modes that can provide uniform color.

Environmental chamber testing

Product coatings and markings must withstand various environmental conditions and must not change during the period of use of the product [1], [14]. In this study, environmental testing was performed in a chamber based on four different operating conditions. Experiments are regularly conducted under temperature and humidity conditions that are not actually expected, such as a combination of extremely low or high temperatures (-40, -20, 40, 100 °C) with high humidity (70%, 90%). This ensures the stability of the samples under normal conditions and also compensates for the short duration of the test exposure (24 hours) compared to the actual operating time. The first test was conducted under ambient conditions with a temperature of -20 °C and a humidity of 70%. The result shows that there is no change in colors or materials after 24 hours in the environmental test chamber as shown in Fig. 15. Optical microscope analyzes did not reveal any damage or defects in the oxide layers.

Figure 15. Color palette after 24 hours of environmental exposure in the test chamber at -20 °C and 70% humidity.

The second test was conducted under ambient conditions with a temperature of -40 °C and a humidity of 90%. The result reveals numerous minor changes to the surface after 24 hours of exposure to the environment in the chamber, as shown in Fig. 16.

Figure 16. Color palette after 24 hours of environmental exposure in the test chamber at -40 °C and 90% humidity.

Photographs of the problem areas and microimages of the defects are shown in Figs. 17a and fig. 17b. A cloudy spot with a diameter of about 400 μm appears on the surface of square No. 1 (Fig. 17a, left). Upon detailed observation under an optical microscope, it was found that the spot is a modified oxide layer with remarkable damage (Fig. 17b left). However, the rest of the square shows no changes. The presence of a stain is probably due to surface contamination or an impurity in the material. The creation of these types of defects is random in nature and occurs only once during the entire test. In square #5, the color changes slightly from blue to gray at the end of the treated area, which may be due to the partial oxidation of the sample (Fig. 17a middle). Under the microscope (Fig. 17b middle), only one damaged area with dimensions of approximately 1 × 1.5 mm is visible. Since these types of defects are characteristic of only one color, it can be concluded that they are probably related to the operating mode of the laser. In square #10, the color changed from burgundy to yellow in an area approximately 1 × 0.5 mm in size (Fig. 17a, right). Microscopic analysis presents the degraded region where the oxide film was etched while the structure was not destroyed (Fig. 17b right). This type of

defect can be caused by high humidity, which is likely to increase with increasing test exposure time. It can be concluded that, in general, laser colored stamps can withstand low temperature and high humidity environmental conditions [3], [15]. However, for these purposes, it is recommended that the color palette be slightly changed.

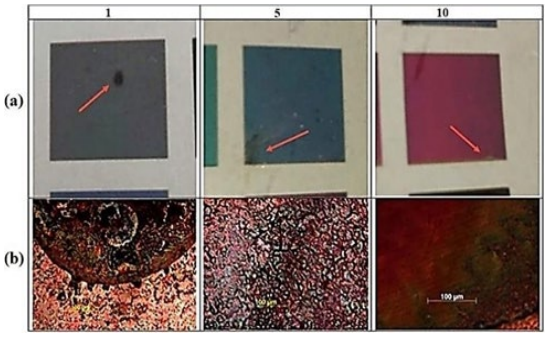

Figure 17. Color errors after 24 h exposure in an environmental test chamber at -40 °C and 90% humidity: a) photographs b) microimages.

The third test was conducted under ambient conditions: temperature 40 °C and humidity 70%. The results showed that the palette had no significant defect and no change in color or metal surface was observed after 24 hours in the environmental test chamber as shown in Fig. 18.

Figure 18. Color palette after 24 hours of environmental exposure in the test chamber at 40 °C and 70% humidity.

However, upon careful inspection, a spot of approximately 1 × 2 mm in size was found in one of the corners of square No. 4, visible only at a certain angle, as shown in Figure 19a. Microscopic analysis shows that the observed spot is a darkening of part of the oxide film, which may be due to the adjustments of the laser processing parameters (Fig. 19b). Overall, the color palette is relatively stable under the environmental conditions of Test 3.

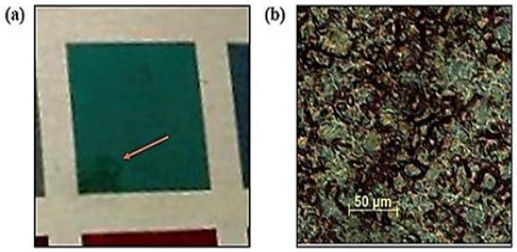

Figure 19. Color error of square No. 4 after 24 h exposure in an environmental test chamber at a temperature of 40 °C and a humidity of 70%: (a) photographs (b) microimage.

The last test was conducted under extremely harsh environmental conditions - temperature 100 °C and humidity 90%. The result showed some spots and dark spots on the metal surface itself and on the colors seen in fig. 20.

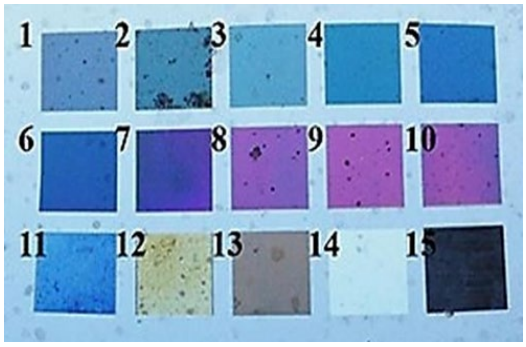

Figure 20. Color palette after 24 hours exposure in the environmental test chamber at a temperature of 100 °C and humidity of 90%.

Most of the obvious defects are presented in Fig. 21a left and center. Almost entire color squares No. 2 and No. 8 are damaged in the form of dark spots with sizes from 500 µm to 3 mm, which do not depend on the laser processing parameters. Optical microscopic analysis of Fig. 21b on the left and fig. 21b right , 21b middle means that the spots appeared are a complete breakdown of the oxide film, most likely caused by the evaporation of the condensed water on the surface due to the humidity/temperature of the test chamber. Furthermore, the untreated surface demonstrates poor resistance to such types of environmental conditions (Fig. 21a) right). When examining the surface with an optical microscope, dark spots ranging from 0.5 to 2 mm in size were found on the entire untreated steel surface (Fig. 21b, right). The darkening may be related to the rusting of certain areas of the surface caused by the condensation and subsequent evaporation of water on the metal, leading to partial oxidation.

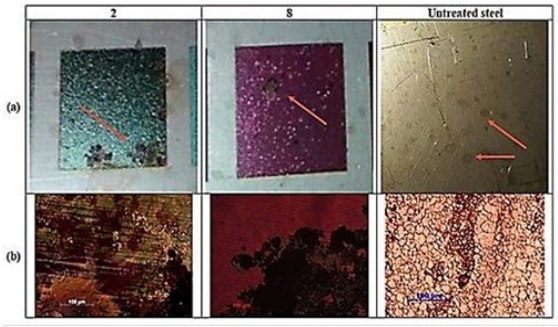

Figure 21. Color errors after 24 h exposure in an environmental test chamber at a temperature of 100 °C and a humidity of 90%: a) photographs b) microimages.

Therefore, the results of the test experiment show that color laser marking is not suitable for application in harsh environmental conditions with very high temperature and humidity. However, if there is adequate air circulation in the workplace, the risk of damage to the colored area can be greatly reduced.

IV. CONCLUSIONS

The stability of color laser marking under different environmental conditions was investigated using a climatic test chamber for four different operating conditions, including low and high temperatures and high humidity [13]. The results showed that the color palette has great persistence in most environmental conditions; however, at excessively high temperature and high humidity (100°C, 90%), limited destruction occurred in some colors and the raw metal surface was also damaged. Also, prolonged exposure to -40°C and 90% humidity results in minor discoloration of many colors that need to be replaced with more stable ones. The mechanical stability of the color palette was evaluated by determining the Vickers hardness value before and after laser treatment using a microhardness tester equipped with a diamond pyramid. After processing, the hardness of most of the samples was on average 26% less than the hardness of the base material, which still confirms the high hardness of the coatings and therefore ensures the mechanical resistance of the color markings against external influences. Moreover, given the fact that the color is not obtained by adding an additional layer of coating, but by changing the surface of the material itself, the cohesion of these labels is much higher than color markings created by conventional methods. The stability of the color palette to various chemical compounds including sulfuric acid, sodium hydroxide, ethanol, surfactant and sodium chloride was investigated. The laser color markings produced have been proven to be resistant to chemicals such as caustic soda, surfactants and alcohol. On the other hand, prolonged interaction with acid solutions and salts can damage the colored characters. Therefore, the interaction of color laser marks with environments containing acidic and salty components should be avoided.

The results of this paper make an impressive contribution to the implementation of color laser marking technology in industry. Future research directions would be to develop a color palette of AISI 304 stainless steel that includes at least 30 different colors, and to increase the marking performance by using stronger lasers and higher frequency modes.

The laser processing system developed for the purpose of this research work is based on a nanosecond ytterbium fiber laser on a multi-axis work piece platform and the ability to move the laser scanning head vertically. In the preliminary phase, the scanning system was calibrated and the specifications of the laser beam at the focal point were determined. To find the appropriate power density value, the distribution of the laser spot on the surface is measured. The dependence of the resulting colors on laser processing parameters, including scan speed, pulse duration, emission power, and pulse repetition rate, was investigated. Based on the analysis, twenty color palettes of AISI 304 stainless steel were developed. Each sample consists of 15 squares of different colors and dimensions of 8×8 mm. The obtained oxide films were examined using optical microscopy and scanning electron microscope (SEM). The surface topology was established using atomic force microscopy (AFM). To evaluate the structure of the obtained oxide films, Raman scattering spectroscopy was performed. Peak analysis showed that four types of oxide compositions were created according to the laser processing parameters. The film consists of two main components: Fe_2O_3 and $FeCr_2O_4$, which is consistent with data previously obtained by other researchers. Color standardization was performed based on the standard of the International Commission on Illumination. Light coordinates in the CIE RGB color space were calculated and reflectance spectra of each color were obtained using spectrophotometric measurements. The results confirm that the created colors have appropriate consistency, brightness and cover approximately all spectral regions. The repeatability of the resulting colors is proven by calculating the delta E value. Overall, the color palette confirms exceptional repeatability, although it is recommended that one particular color be replaced as it does not meet the minimum delta requirement.

V. ACKNOWLEDGMENTS

I express my gratitude to Professor Lyubomir Lazov for the dedicated work during these 10 years to deepen the cooperation between the two educational institutions, for the dedication in working with the trainees from the Vasil Levski National Military University and for the knowledge, experience and skills imparted.

I also thank the managements of both institutions over the years for their benevolent attitude and for the opportunity to conduct joint activities.

REFERENCES

[1] Dave Ahearn, ONR Laser Power Jumps 10 Fold; Further 10 - Fold Leaps Seen, Defense Today, August 4, 2004, p. 4

[2] N. Todorov, Lyubomir L., Shterev I.J., Dimitrov N.D. and Ivanov L.L. 2019 Study of cutting and labeling of polymethylmethacrylate using a CO_2 laser Vide. Tehnologija. Resursi -Environment, Technology, Resources. ISBN 1691-5402, Vol 3, 20-22.06.2019 Rezekne, Latvia pp. 37-40.

[3] S. E Lamberson, The airborne laser, Proc. SPIE, Gas Chem. Lasers, vol. 2702, pp. 2702-1_2 702 - 6, Mar. 1996

[4] W. Zhang, Xiao Z. and Yan Z. 1976 Design of online laser marking system by vision guided based on template matching Journal of Physics: Conference Series 1976 012047

[5] L. Lazov, H. Deneva, E. Teirumnieka, Influence of Defocus Position on Laser Cutting Process in Sheet Steel, Environment. Technology. Resources, Rezekne, Latvia Proceedings of the 11 th International Scientific and Practical Conference. Volume III, 163-167,

[6] L. Lazov, Dolchinkov N., Shterev J., Peneva M. and Bozhanova D. 2019 Study of laser cutting and marking on the filt with the help of a CO_2-laser Vide. Tehnologija. Resursi - Environment, Technology, Resources, ISBN 1691-5402, Vol 3 pp. 143-147.

[7] L. Lazov, Angelov N., Teirumnieks E. and Teirumnieka E. 2019 Preliminary numerical analysis for the role of speed onto laser technological processes Vide. Tehnologija. Resursi - Environment, Technology, Resources 3 pp 137-142.

[8] N. Petrov, Optimization of the marking process with laser radiation of samples of tool steel, dissertation, Gabrovo, 2011.

[9] N. Dolchinkov, Lazov L., Shterev Y., Lilianova St. and Pacejs A. 2019 Use of CO_2 laser for marking and clearing of textile materials for manufacture of military equipment 12th International Scienfic and Practical conference Environment. Technology. Resources. 3, ISBN 1691-540206.2019, Rezekne, Latvia, 32-36

[10] N. Todorov, 2020 Practical research of marking and cutting of textiles with increased resistance, using CO_2 laser Journal of Physics: Conference Series 1681 012014, doi:10.1088/1742-6596/1681/1/012014, Online ISSN: 1742-6596, Print ISSN: 1742-6588

[11] S.-T. Tse and Kan C.-W. 2020 Effect of laser treatment on pigment printing on denim fabric: low stress mechanical properties Cellulose 27 10385-10405

[12] N. T. Dolchinkov 2022 Marking and Cutting of Non-metallic Products with CO_2 Laser, J. Phys.: Conf. Ser. 2224 012028 DOI 10.1088/1742-6596/2224/1/012028H, doi: 10.1109/Lighting49406.2021.9599072, Electronic ISBN:978-1-6654-3792-9, CD:978-1-6654-3791-2

[13] L. Lazov, Angelov, N., Teirumnieks, E., ...Pacejs, A., Teirumnieka, Ē., Laser ablation of paint coatings in industry, Vide. Tehnologija. Resursi - Environment, Technology, Resources, 2021, 3, pp. 187–194

[14] E. Teirumnieka, Blumberga, D., Teirumnieks, E., Stramkale, V., Product-oriented production of industrial hemp according to climatic conditions, Agronomy Researchthis link is disabled, 2021, 19(4), pp. 2026–2036

[15] L. Lazov, Teirumnieks, E., Angelov, N., Yankov, E., Modification of the roughness of 304 stainless steel by laser surface texturing (LST), Laser Physicsthis link is disabled, 2023, 33(4), 046001

[16] V. Hristov, Lazov, L., Yankov, E., ...Minev, R., Angelov, N., Investigation of the laser effect of micromechanical properties of stainless steel AISI 304 during the marking process, 2021 6th Junior Conference on Lighting, Lighting 2021 - Proceedings, 2021

[17] N. Padarev, Investigation of Damage from Radiological Dispersal Device, International Journal of Innovative Technology and Interdisciplinary Sciences, 5(4), 2022, pp. 1052–1059. https://doi.org/10.15157/IJITIS.2022.5.4.1052-1059.

[18] N. Padarev, Guidelines for improving laser targeting device in military. Technology transfer: fundamental principles and innovative technical solutions, 2022, 38-40. doi: https://doi.org/10.21303/2585-6847.2022.002681

[19] L. Lazov, N. Padarev, Laser Safety in Army Education, Revista, Vol. XXVIII, Nr. 1 (109), ED. Academiei Forţelor Terestre „Nicolae Bălcescu" Sibiu, Romania 2023, ISSN 2247-840X, ISSN-L = 1582-6384, pp. 61–68, DOI: 10.2478/raft-2023-0009

[20] N. Padarev, Analysis of the Relation Between Climate Changes and Security Area, International Conference Knowledge-Based Organization, Vol. XXIV. Conference proceedings 3, Applied technical Sciences and Military Technologies, Sibiu, Rom., 2018, pp 169-173, ISSN 1843-682X, ISBN 978-973-153-329-2.

[21] L. Lazarov, Perspectives and trends for the development of electronic warfare systems, International Conference on Creative Business for Smart and Sustainable Growth, CreBUS 2019, 2019, 8840074

[22] S. Stoykov, Dimitrova, S., Marinov, R., The development of educational capacity of human resources in the field of security-main priority of national security, International Conference on Creative Business for Smart and Sustainable Growth, CreBUS 2019, 2019, 8840062